EurJOC
European Journal of Organic Chemistry

Research Article
doi.org/10.1002/ejoc.202400783

Chemistry Europe
European Chemical Societies Publishing

www.eurjoc.org

Characterization and Optimization of the Photoluminescent Properties of Imidazo[1,5-*a*]quinolines

Niclas Kulhanek,[a] Kateryna V. Borysova,[b] Michael Kirchner,[a] Klaus Müller-Buschbaum,[b] and Richard Göttlich*[a]

In our previous work we could show, that Imidazo[1,5-*a*]quinolines are compounds with interesting optical properties. In this work, we optimized the photoluminescent properties of imidazo[1,5-*a*]quinolines by following outlined trends in our previous work. By introducing electron-rich and electron-poor residual groups on the imidazole ring, the quantum yield (QY) could be significantly increased. This indicated a clear advantageous substitution pattern for this system. In addition, cyclic voltammetric and UV/vis measurements in solid state lay the foundation for applications, such as organic light-emitting diodes (OLEDs).

Introduction

Modern display and lighting technology are increasingly dominated by OLEDs. Since their introduction by Tang and VanSlyke, they were developed and improved greatly in terms of efficiency.[1] Different strategies have been pursued to increase the internal quantum efficiency (IQE), resulting in a large number of green and red emitter materials with good IQEs and stability.[2] The development of molecules with blue emission was particularly challenging. Most of these blue emitter materials have a short lifetime and lower efficiency, as the required band gap of approximately 3 eV leads to long exciton lifetimes (μs). The resulting hot exciton states can decompose the emitter material and thus shorten the lifetime of the entire OLED.[3] Therefore, the development of new organic molecules with blue emission and high stability is an important contribution to an illuminated future.[4]

Blue emission combined with stability is therefore rare in organic molecules.[5] Imidazo[1,5-*a*]*N*-heteroaromatic ring systems are a structural motif frequently incorporated in pharmacologically and biologically active agents and are also found in natural products.[6] Imidazo[1,5-*a*]pyridines in particular have proven to be materials for various applications, such as in nonlinear optics (NLO), confocal microscopy or fluorescence sensing.[7,8] In addition, these simple molecules have uncommon photophysical properties. Some imidazo[1,5-*a*]pyridines have a strong blue emission with a good quantum yield (QY) and a large Stokes shift.[8–11] Especially as ligands, they have already been incorporated into many complexes and successfully implemented into an optical device by Weber *et al.*[12] A less studied but promising subclass are the imidazo[1,5-*a*]quinolines, which possess similar photophysical properties and will be the focus of this work (Scheme 1).

In our group, we have already investigated some imidazo[1,5-*a*]quinolines and found that this class not only showed a strong blue emission with better QY, but was also more stable than imidazo[1,5-*a*]pyridines (Scheme 1).[13] Imidazo[1,5-*a*]quinolines proved to have high stability under physical vapor deposition conditions and the increase in melting point temperature simplifies their implementation as emitter materials in this process. We were able to successfully integrate one of these molecules into an OLED and consequently investigated the influence of various residual groups on the QY.[14] In a large-scale screening, we could identify a preferred substitution pattern.[15] On the one hand, combinations of aromatic electron-rich residues in R^2-position and electron-poor residues in R^1-position lead to increased QY. Particularly advantageous in the R^1-position proved to be *N*-heteroaromatic substituents, i.e. 2-pyrimidinyl in this position lead to a very high QY. On the other hand, a slight steric influence of groups in R^2-position on the QY could be observed. In this work, we will continue these studies towards steric influences on the QY by introduction of sterically demanding electron-rich residues in R^2 and conduct further measurements

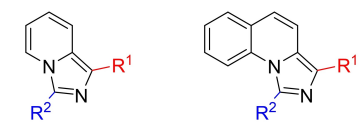

imidazo[1,5-*a*]pyridines imidazo[1,5-*a*]quinolines

Scheme 1. General structures for imidazo[1,5-*a*]pyridines and imidazo[1,5-*a*]quinolines.

[a] *N. Kulhanek, M. Kirchner, R. Göttlich*
Institute of Organic Chemistry, Justus-Liebig-University, Heinrich-Buff-Ring 17, 35392 Giessen, Germany
E-mail: Richard.Goettlich@org.chemie.uni-giessen.de

[b] *K. V. Borysova, K. Müller-Buschbaum*
Institute of Inorganic Chemistry, Justus-Liebig-University, Heinrich-Buff-Ring 17, 35392 Giessen, Germany

Supporting information for this article is available on the WWW under https://doi.org/10.1002/ejoc.202400783

Research Article
doi.org/10.1002/ejoc.202400783

to characterize this class of molecules and improve their optical properties.

Results and Discussion

Synthesis of the imidazo[1,5-*a*]quinolines

On the basis of the highlighted trends, we applied a synthetic route that we already presented in an earlier publication (Scheme 2).[15] In this route we started from 2-aminomethylquinolin dihydrochloride 1, which is available *via* a two steps synthesis known from literature.[16] Compound 1 was reacted with acid chloride R^2COCl and the resulting amides 2 were cyclized with Tf_2O.[17] To study steric effects, sterically large and electron-rich aromatic systems were chosen as R^2. While the cyclization with 9-anthryl and OPh could be performed well, the amides of 9H-carbazole-9-yl and 10H-phenothiazine-10-yl were prone to decomposition which lead to a lower yield of cyclized products 3c and 3 d. The subsequent bromination with NBS could be achieved in excellent yields with all systems.

The obtained bromides **4** were coupled with 2-bromopyrimidine *via* Negishi coupling (Scheme 3 route 1) and since OPh proved to be a particularly good substituent in the subsequent measurements, **4 b** was combined with a large number of electron-poor aromatic compounds. The introduction of a 2-*s*-triazinyl residue *via* this coupling route is impractical, as the corresponding halides are commercially not available. Therefore, *s*-triazine was reacted directly with the lithiated bromide **4 b** and the resulting dihydro-*s*-triazine was aromatized with DDQ to form the product **6 c** (Scheme 3 route 2).[18]

The Negishi coupling lead in most cases to very good yields of the desired products (Scheme 4), only sterically very demanding substrates lead to reduced yields. Thus, sterically demanding residues in position R^2 obstruct the coupling for **7-10 b**. To enlarge the scope, bromides from one of our earlier works were included.[19] The newly developed substitution with *s*-triazine was also achieved with very good yields.

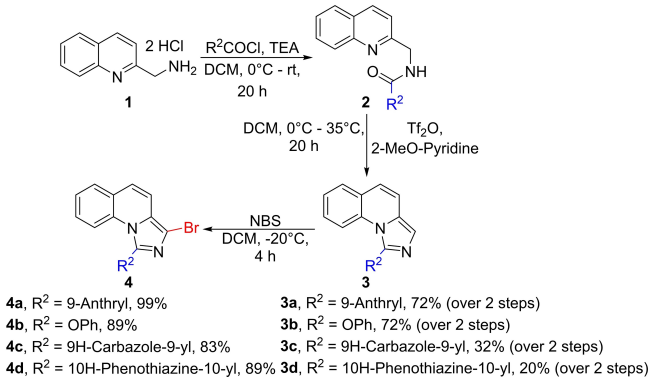

4a, R^2 = 9-Anthryl, 99%
4b, R^2 = OPh, 89%
4c, R^2 = 9H-Carbazole-9-yl, 83%
4d, R^2 = 10H-Phenothiazine-10-yl, 89%
3a, R^2 = 9-Anthryl, 72% (over 2 steps)
3b, R^2 = OPh, 72% (over 2 steps)
3c, R^2 = 9H-Carbazole-9-yl, 32% (over 2 steps)
3d, R^2 = 10H-Phenothiazine-10-yl, 20% (over 2 steps)

Scheme 2. General synthetic route for the cyclisation and bromination of the new imidazo[1,5-a]quinolines.

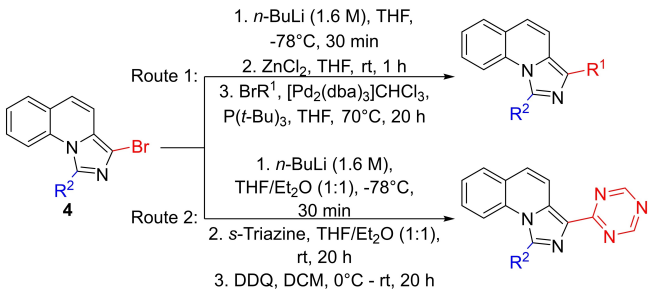

Scheme 3. Subsequent reaction of the bromides 4 in a Negishi coupling *via* route 1 and a substitution with *s*-triazine *via* route 2.

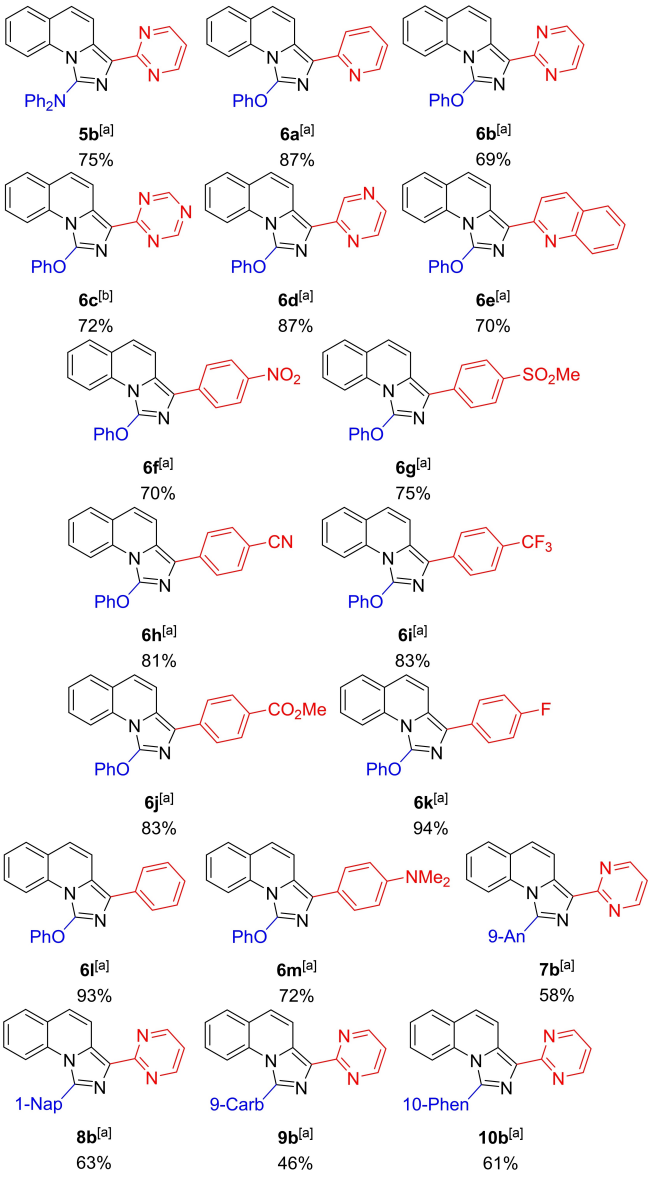

Scheme 4. Isolated Yields for all new final products. [a] Route 1 see scheme 1, [b] Route 2 see scheme 1. (9-An = 9-Anthryl, 1-Nap = 1-Naphthyl, 9-Carb = 9H-Carbazole-9-yl, 10-Phen = 10H-Phenothiazine-10-yl).

Research Article
doi.org/10.1002/ejoc.202400783

Chemistry Europe
European Chemical Societies Publishing

Photophysical Measurements in Liquid Phase

Optical measurements were conducted using a 0.1 μM chloroform solution at room temperature. A 0.1 μM solution of quinine sulfate in 0.5 M H_2SO_4 was used as the reference.[20] The fluorescence QY was calculated as described in the literature.[21] All measurements were performed under air. The extinction and emission spectra as well as molar extinction coefficients log ε of all measured compounds are provided in the supporting information.

The measurements of the extinction with different residues in R^2-position showed that all compounds had a maximum around 369 nm (Scheme 5). This observation could also be validated for the emission, as almost all systems displayed a blue emission at about 450 nm (Figure 1 top). The only compound that differed greatly was **7b**, which had a slight cyan coloration. Larger differences could be observed in the QY. The increase of the residue in R^2 from the base system **11b** to **8b** and **9b** first displayed an increase from 33% to 40% when naphthyl was introduced. However, this was almost halved to only 22% by the enlargement of the R^2-position to 9-anthryl in **7b**. The strongest increase was observed when an oxygen- or nitrogen-center was introduced as a link between the residue and the imidazole ring. Here, **5b** displayed a QY of 66% and **6b** with 85% a significantly higher QY than our best compound so far, **14b**. Direct linkage of the phenyl residues in **5b** to carbazole in **9b** yielded an increase of the QY to 81%, while bridging with sulfur in **10b** almost completely canceled the emission. From these data, it is evident that a purely sterically demanding residue in the R^2-position is disadvantageous, as none of the new compounds with solely large R^2 residues showed a significantly better QY than **14b**. This changes when a heteroatom is used as a linker, resulting in significantly different QY.

Since the OPh residue proved to be the best group in R^2-position, an attempt was made to identify other suitable electron-poor residues in the R^1-position. The extinction varied greatly with the different residual groups (Scheme 6). The strongly electron-withdrawing nitro group in particular resulted in a strong bathochromic shift. In contrast, the emission of the other studied compounds remained largely at a value of approximately 460 nm (Figure 1 top). Likewise, the nitro group led to a significant deviation in the emission wavelength. By

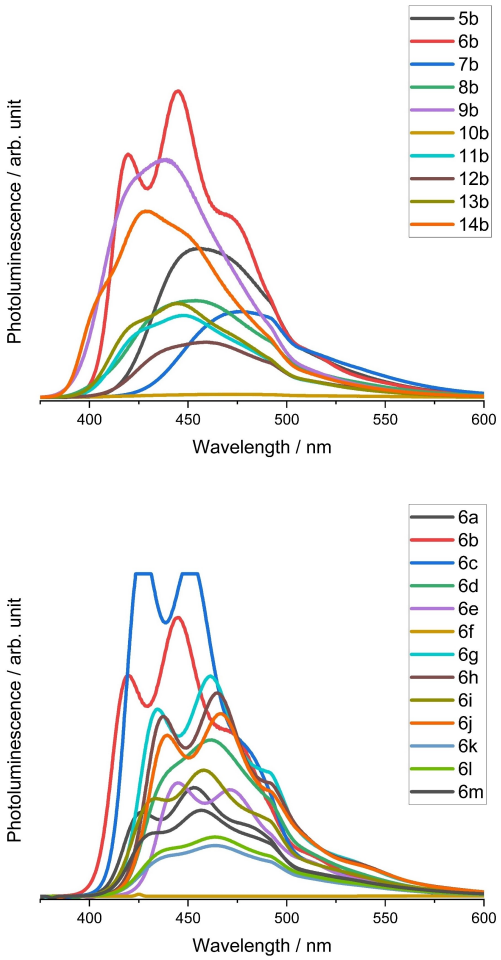

Figure 1. F-Spectra for different rests in R^2-position and 2-pyrimidinyl in R^1-position (top) and different rests in R^1-position and OPh in R^2-position (bottom). Measured at 25 °C, under air, 0.1 μM solution in $CHCl_3$ and with the extinction maxima as excitation wavelength.

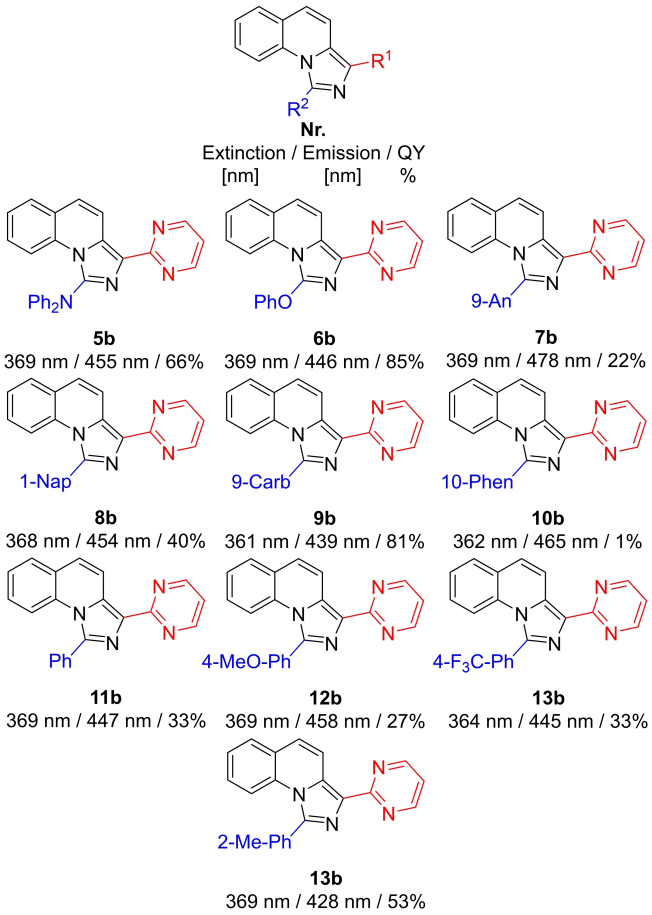

Scheme 5. Extinction, Emission maximas and calculated QYs for different rests in R^2-position and 2-pyrimidinyl in R^1-positions. Measured at 25 °C, under air, 0.1 μM solution in $CHCl_3$ and with the extinction maxima as excitation wavelength. (9-An = 9-Anthryl, 1-Nap = 1-Naphthyl, 9-Carb = 9H-Carbazole-9-yl, 10-Phen = 10H-Phenothiazine-10-yl)

Research Article
doi.org/10.1002/ejoc.202400783

Chemistry Europe
European Chemical Societies Publishing

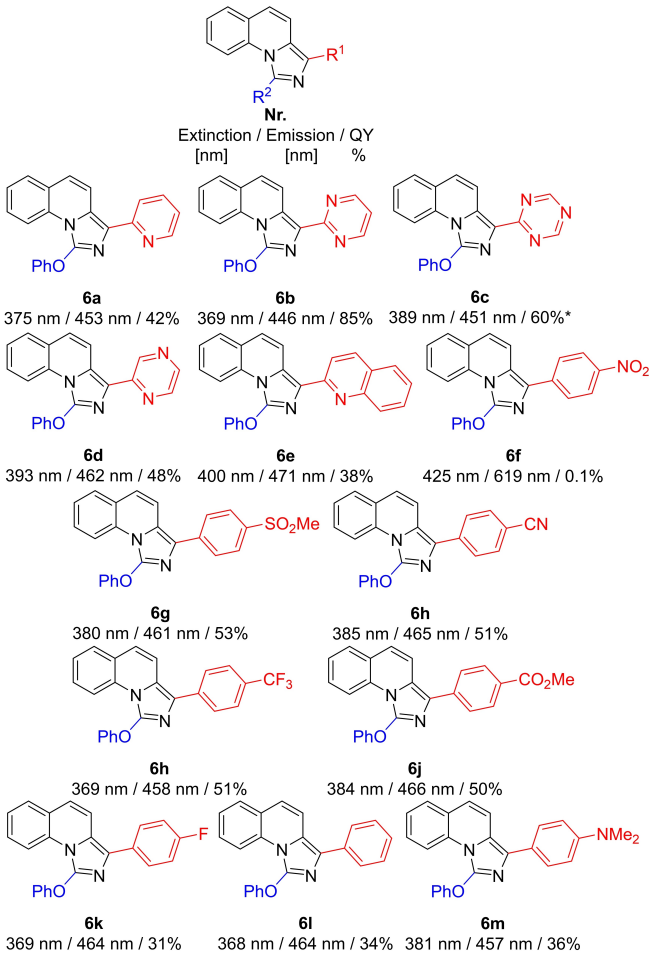

Scheme 6. Extinction, Emission maximas and calculated QYs for different rests in R^1-position and OPh in R^2-positions. Measured at 25 °C, under air, 0.1 μM solution in $CHCl_3$ and with the extinction maxima as excitation wavelength. * Emission could not be fully measured. QY calculated with the incomplete measured Emission.

substitution of the carbon in 2-position of the phenyl ring with more nitrogen, the QY could be greatly increased compared to **6l** from 34% to **6a** with 42%, up to **6b** with 85%. The influence of the substitution pattern of the residues was demonstrated by the introduction of 2-pyrazinyl **6d** for which we observed a decreased QY of 48% compared to **6b**. Enlargement of the *N*-heteroaromatic system size also resulted in a decrease in QY, as can be observed for **6e**. Showing that a sterically small substituent is also advantageous in R^1-position. Surprisingly, the QY with a *s*-triazinyl residue could not be increased any further. Although **6c** had such a strong emission that it could not be fully measured, it also had a higher molar extinction coefficient (Figure 1 bottom). It can also be observed that all phenoxy based systems **6** have a characteristic second weak emission maximum before the main maximum. As the *para*-substitution proved to be the most effective for phenyl, only these were synthesized.[15] The substitution with dimethylamine **6m** and fluorine **6k** in *para*-position did not show any significant change. Dimethylamine had proven to be the only exception for +M substituents in our previous work.[15] This substitution of compounds **6m** and **6k** did only result in minor changes of the QY compared to **6l**. By increasing the electron-withdrawing effect to a methyl ester **6j**, the QY could be improved to 50%. However, it could not be increased above this value by further increasing the electron withdrawing effect of the substituent in *para*-position to trifluoromethyl **6i**, nitrile **6h** and methylsulfonyl **6g**. Substitution with a nitro group completely extinguished the emission. This quenching effect of photo emissions between 450–630 nm is well known from literature.[22]

Increasing the electron deficiency through *para*-substitution alone proved to be insufficient. The strongest improvement was observed with the substitution of the carbon in 2-position of the phenyl ring with more nitrogen, with the 2-pyrimidinyl residue being the best substituent in the R^1-position. It is possible that this results in a less hindered rotation of the substituent in the R^1-position leading to a better interaction between the residue in R^1-position and the imidazole ring core.

In general, it is surprising that the imidazo[1,5-*a*]quinolines retained their blue emission in almost all cases, while imidazo[1,5-*a*]pyridines showed a wide variety of emission wavelengths due to substitutions with a wide variety of functional groups.[11] Comparable imidazo[1,5-*a*]pyridines systems achieved QYs between 7–50% and emission between 430–480 nm.[10,13,23] Similar properties were observed forimidazo[5,1-*a*]isoquinolines, which also show an emission range of 430–450 nm and 5–48% QY.[24] While the emission range and pattern are the same compared to imidazo[5,1-*a*]isoquinolines and imidazo[1,5-*a*]pyridines, we were able to significantly increase the QY to over 80% with the substitution with 2-pyrimidinyl and other *N*-heterocycles.

Photophysical Measurements in Solid Phase

For comparison, absolute QYs (s) were determined in the solid state under air at 25 °C by measuring each sample as well as a reference material several times (4 times sample/3 times reference) with subsequent calculation of QY value (an average value) and standard deviation that represents the measurement error. Magnesium oxide was utilized as a reference material.

Due to the preparative complexity, only molecules that already exhibited sufficient emission and QY in solution were measured. For this reason, **5b**, **6a**, **6b**, **6c**, **6g** and **9b** were selected. Unexpectedly, despite showing strong emission in solution, **6a** and **9b** did not possess a sufficiently high emission in their solid state for the measurements and were excluded. The UV/vis and F maxima shifted approximately 50 nm towards the red spectrum for the measured systems (Scheme 7). Noteworthy here is **6b**, as a very strong shift in extinction and emission was observed (Figure 2). Compound **6b** also lost over 60% of its QY (s) compared to the liquid phase, while **5b** only displayed a reduction of 30%. Molecules **6c** and **6g** could not exceed 15% QY (s). The comparatively weak emission of **6c** was particularly surprising, as it emitted exceptionally strongly in solution. It can be concluded that 2-pyrimidinyl is a very good substituent for the R^1-position even in the solid phase. However,

Research Article
doi.org/10.1002/ejoc.202400783

Chemistry Europe
European Chemical Societies Publishing

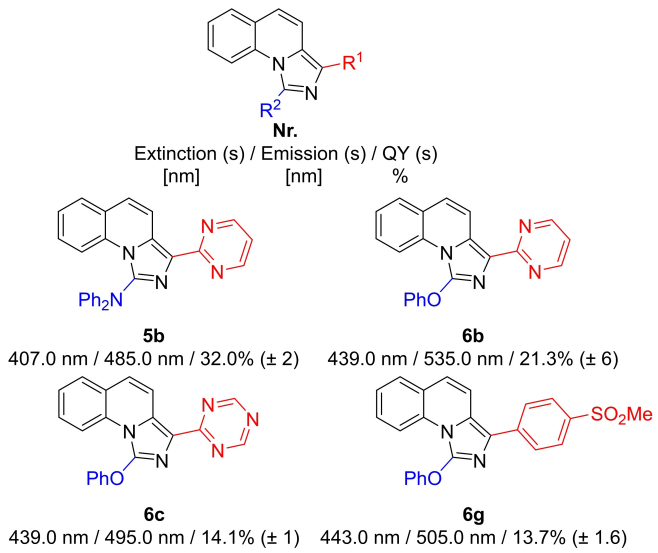

Scheme 7. Extinction, Emission maximas and calculated QYs (s) in solid state for the measured systems. Measured under air and 25 °C (5b, λ_{ex} = 330 nm; 6b, λ_{ex} = 360 nm; 6c, λ_{ex} = 360 nm; 6 g, λ_{ex} = 415 nm).

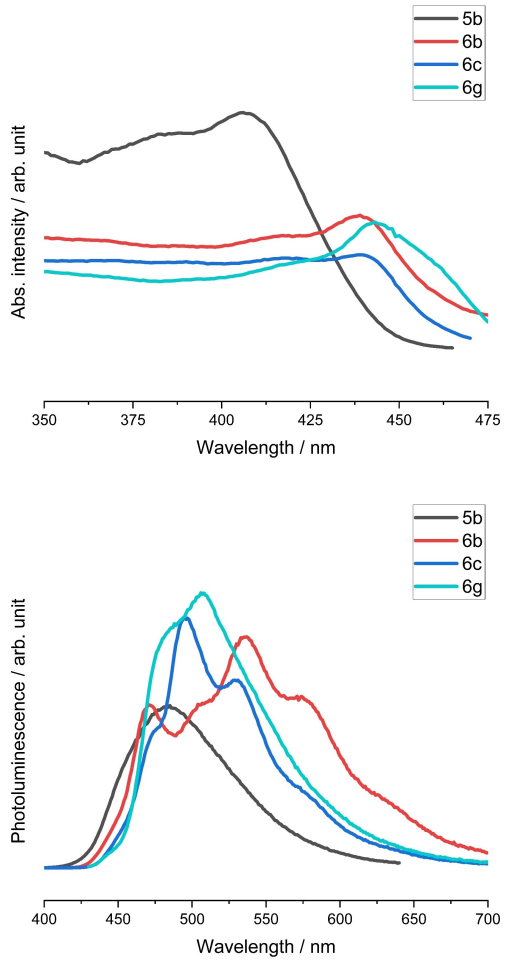

Figure 2. UV/vis (top) and F-Spectra (bottom) in solid state for the measured systems at 25 °C and under air (black **5 b**, λ_{ex} = 330 nm; red **6 b**, λ_{ex} = 360 nm; blue **6 c**, λ_{ex} = 360 nm; cyan **6 g**, λ_{ex} = 415 nm).

the QY (s) loss in **5 b** was mitigated to a greater extent than in **6 b**.

Cyclic Voltammetric Measurements and DFT-Calculations

Cyclic voltammetry (CV) measurements were performed with a glassy carbon electrode as working electrode, a platinum/titanium electrode as counter electrode and an Ag/AgCl reference electrode. The HOMO energy was estimated by using this literature procedure with ferrocene as standard[25] and the LUMO energy was calculated from the HOMO energy and the bandgap (BG) energy, which was obtained by a linear fit of the extinction edge and conversion of the intersection wavelength into an energy value.[26] The 5 mM sample solution was dissolved in a 0.1 M tetrabutylammonium tetrafluoroborate DMF-solution, measured at 25 °C, under inert atmosphere.

All density functional theory computations were carried out using the Orca 5.0.3 program package. For structural optimizations and the acquisition of HOMO and LUMO energies, the B3LYP hybrid functional[27] with the Karlsruhe basis set def2-TZVP[28] was deployed. The D3 scheme[29] with Becke-Johnson dampening[30] was used to account for dispersion interactions.

The 2-pyrimidinyl substituted systems displayed all very similar results in the CV measurements. A reversible oxidation could be shown for all substances without a reduction being measured (Figure 3 top). Only **5 b** showed two oxidation maxima, but again without reduction. With OPh in R^2-position, two oxidation maxima were measured with **6 f**, **6 i**, **6 k** and **6 l** whereas the other systems showed only one oxidation maximum (Figure 3 bottom). An exception is **6 m**, which not only displayed two oxidation maxima, but also two reduction maxima. This could explain the unique properties of **6 m**, as it is the only electron-rich substituent that has high QYs.

Non-reversible oxidation distinguishes the imidazo[1,5-*a*]quinolines from the imidazo[1,5-*a*]pyridines, which typically show reversibility of oxidation. Moreover, the potential of the imidazo[1,5-*a*]quinolines at around 1.3 V is considerably higher than that of the imidazo[1,5-*a*]pyridines at approximately 0.4 V.[10,13]

Energy levels for HOMO is consistent at below −5 eV, with 2-pyrimidinyl substituted system tending more towards < −5.5 eV (Table 1). Very large systems **7 b** and **10 b** and heteroatom-linked systems **5 b** and **6 b** show slightly higher HOMO energies. This trend can also be observed for LUMO Energies. While most systems are around −2.5 eV, the systems mentioned above show slightly higher energies. The HOMO and LUMO energies are similar to those of the imidazo[1,5-*a*]pyridines.[10,13] This results in a consistent BG of 3 eV for 2-pyrimidinyl substituted systems, with the remaining systems having a BG below 3 eV.

The DFT calculations showed very good agreement with HOMO energies, while LUMO energies deviated strongly (Table 2). This discrepancy in the use of this approach is well known in the literature.[31] However, it can be observed that these deviations are constant at around +0.6 eV. This excess also resulted to higher values for BG energies, which remained

Research Article
doi.org/10.1002/ejoc.202400783

Chemistry Europe
European Chemical Societies Publishing

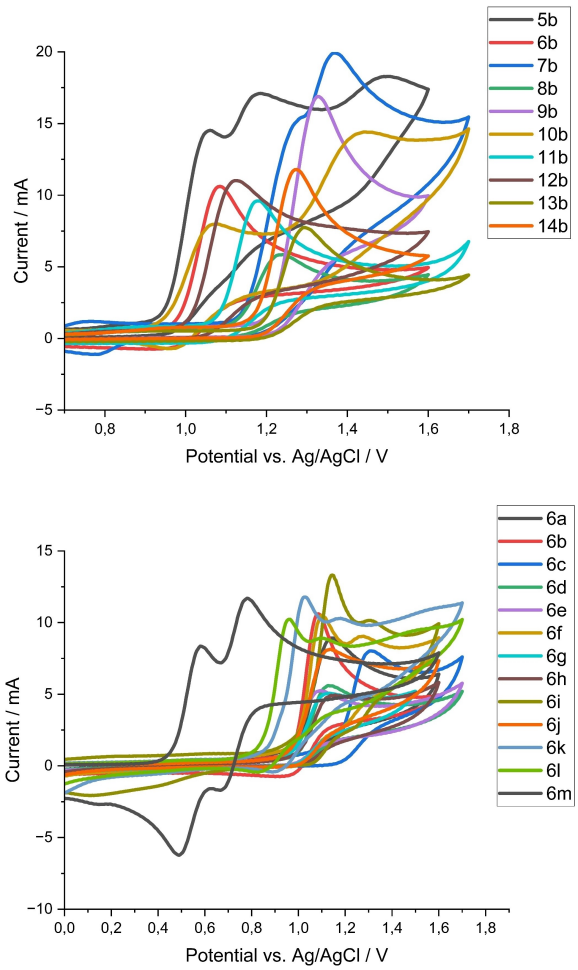

Figure 3. CV-Spectra for different rests in R^2-position with 2-pyrimidinyl in R^1-position (top) and for different rests in R^1-position with OPh in R^2-position (bottom). Measured at 25 °C, under inert atmosphere, 5 mM sample-solution dissolved in a 0.1 M tetrabutylammonium tetrafluoroborate DMF-solution, at a scan rate of 200 mVs^{-1}.

constant at around 3.5 eV for all systems. An exception to this was **6f**, which also had a small BG in the CV measurement.

Conclusions

We were successful in expending on the trends we observed for the 1,3-substitution of imidazo[1,5-a]quinolines. By introduction of sterically large heteroatom-linked residues in the R^2-position and combination with *N*-heteroaromatics in the R^1-position. In particular, the use of diphenylamine or phenyl ether in conjunction with 2-pyrimidinyl increased the QY to over 80% in solution. The best system in solution was **6b** with 86% QY. While in the solid phase **5b** with 32% displayed the highest QY (s) compared to the other systems. By CV measurements it could also be determined that all systems possess a BG of about 3 eV, with HOMO and LUMO energies varying only slightly between different substitutions. In summary we were able to develop and prepare new imidazo[1,5-a]quinolines that show a high fluorescence quantum yield in solution as well as in the solid state. Further experiments towards applying these new emitter molecules for OLED applications are currently performed in our group.

Experimental Section

All solvents were purified by distillation prior to use. Anhydrous solvents were used from ACROS Organics™ as AcroSeal™ bottles. Commercially available chemicals were used as obtained from the supplier, unless otherwise stated. Syntheses prepared under anhydrous conditions were generally performed using standard Schlenk technique in nitrogen atmosphere. For purification by column chromatography, silica gel 60 (Merck) was used. ^1H and ^{13}C NMR spectra were recorded on the Bruker Avance II 400, the Bruker Avance III 400 and the Bruker Avance II 200 "Microbay" spectrometers in deuterated solvents. ^1H and ^{13}C chemical shifts were determined by reference to the residual solvent signals. High-resolution ESI mass spectra were recorded in methanol with an ESImicroTOF spectrometer from Bruker Daltonics in positive ion mode, unless otherwise stated. As a power supply, the Sky Toppower PS1110 was used. Melting points were determined with a Gallenkamp Melting Point Apparatus. The CHN elemental analysis was performed using the CHN-Analysator: Thermo Flash EA-1112 Series. UV-vis extinction in solution was measured with an Analytik Jena Specord 200 Plus spectrometer and fluorescence emission data were obtained from a Jasco Germany FP 8300 spectrometer. Cyclic voltammetry measurements were performed with a glassy carbon electrode as working electrode, a platinum/titanium electrode as counter electrode and an Ag/AgCl reference electrode. Ferrocene was used as standard and the electrochemical data were recorded with an e-corder 410 eDAQ (eDAQ, Colorado Springs, US) and the program eChem. Solid-state photoluminescence properties were studied on Horiba Jobin Yvon Fluorolog 3 equipped with 450 W xenon lamp as a light source, double-grated monochromators (emission and excitation) and photomultiplier tube R928P (Horiba). FluorEssence software by Horiba was used to carry out the measurements. Quantum yield (QY (s)) for solid samples was measured using previously mentioned Horiba Jobin Yvon Fluorolog 3 combined with a Quanta-Phi integrating sphere F-3029 (by Horiba). Magnesium oxide was utilized as a reference material.

General procedure for imidazole ring closure adapted from Pelletier *et al.*[17]:

60 mL of dry DCM was added to 2-(aminomethyl)quinoline dihydrochloride 1 (1 eq) under N_2 atmosphere. The suspension was cooled to 0 °C and dry TEA (3.4 eq) was added. The yellow solution was kept at 0 °C for 30 min. Acid chloride R^2COCl (1.1 eq) was added, and the solution was stirred for 20 h at room temperature. Finally, 60 mL sat. Na_2CO_3 solution was added, and the aqueous phase was extracted twice with 60 mL DCM. The combined organic phases were dried over Na_2SO_4, filtered, and the solvent removed *in vacuo*. The crude quinoline amide 2 (1 eq) was placed in 60 mL of dry DCM under N_2 atmosphere and cooled to 0 °C. The solution was first treated with 2-methoxypyridine (1.1 eq), followed by slow addition of Tf_2O (1.2 eq). The reaction solution was stirred at 35 °C for 20 h. Then, 20 mL sat. Na_2CO_3 solution was added slowly, and the aqueous phase was extracted twice with 60 mL DCM. The combined organic phases were dried over Na_2SO_4, filtered and the solvent removed *in vacuo*. Purification was carried out by silica chromatography.

General procedure for bromination:

The imidazo[1,5-*a*]quinoline 3 was placed in 60 mL dry DCM under N_2 atmosphere and cooled to −20 °C. 1.1 eq NBS was slowly added

Research Article
doi.org/10.1002/ejoc.202400783

Table 1. CV–Data for different rest at R^2 and R^1-position. Measured at 25 °C, under inert atmosphere, 5 mM sample-solution dissolved in a 0.1 M tetrabutylammonium tetrafluoroborate DMF-solution.

Nr.	R^2	R^1	HOMO/eV	LUMO/eV	BG/eV
5b	NPh_2	2-Pyrimidinyl	−5.27	−2.30	2.97
6b	OPh	2-Pyrimidinyl	−5.33	−2.37	2.97
7b	9-Anthryl	2-Pyrimidinyl	−5.26	−2.20	3.06
8b	1-Naphthyl	2-Pyrimidinyl	−5.56	−2.51	3.06
9b	9H-Carbazole-9-yl	2-Pyrimidinyl	−5.59	−2.47	3.12
10b	10H-Phenothiazine-10-yl	2-Pyrimidinyl	−5.26	−2.23	3.03
11b	Ph	2-Pyrimidinyl	−5.56	−2.53	3.03
12b	4-MeO-Ph	2-Pyrimidinyl	−5.45	−2.49	2.97
13b	4-F_3C-Ph	2-Pyrimidinyl	−5.64	−2.60	3.03
14b	2-Me-Ph	2-Pyrimidinyl	−5.59	−2.52	3.07
6a	OPh	2-Pyridinyl	−5.33	−2.74	2.59
6c	OPh	2-*s*-Triazinyl	−5.26	−2.39	2.87
6d	OPh	2-Pyrazinyl	−5.26	−2.45	2.81
6e	OPh	2-Quinolinyl	−5.26	−2.73	2.53
6f	OPh	4-O_2N-Ph	−5.36	−2.93	2.43
6g	OPh	4-MeO_2S-Ph	−5.31	−2.48	2.83
6h	OPh	4-NC-Ph	−5.33	−2.52	2.81
6i	OPh	4-F_3C-Ph	−5.29	−2.42	2.87
6j	OPh	4-MeO_2C-Ph	−5.28	−2.48	2.81
6k	OPh	4-F-Ph	−5.17	−2.35	2.82
6l	OPh	Ph	−5.16	−2.34	2.83
6m	OPh	4-Me_2N-Ph	−4.92	−2.10	2.81

Table 2. DFT-Calculation results for HOMO/LUMO of the specific molecules.

Nr.	R^2	R^1	theo. HOMO/eV	theo. LUMO/eV	theo. BG/eV
5b	NPh_2	2-Pyrimidinyl	−5.21	−1.74	3.47
6b	OPh	2-Pyrimidinyl	−5.28	−1.77	3.51
7b	9-Anthryl	2-Pyrimidinyl	−5.41	−2.04	3.37
8b	1-Naphthyl	2-Pyrimidinyl	−5.41	−1.73	3.68
9b	9H-Carbazole-9-yl	2-Pyrimidinyl	−5.64	−1.85	3.79
10b	10H-Phenothiazine-10-yl	2-Pyrimidinyl	−5.31	−1.80	3.51
11b	Ph	2-Pyrimidinyl	−5.39	−1.77	3.62
12b	4-MeO-Ph	2-Pyrimidinyl	−5.25	-1.70	3.55
13b	4-F_3C-Ph	2-Pyrimidinyl	−5.61	−1.97	3.64
14b	2-Me-Ph	2-Pyrimidinyl	−5.43	−1.72	3.71
6a	OPh	2-Pyridinyl	−5.22	−1.58	3.64
6c	OPh	2-*s*-Triazinyl	−5.58	−2,11	3,47
6d	OPh	2-Pyrazinyl	−5.37	−1.79	3.58
6e	OPh	2-Quinolinyl	−5.24	−1.79	3.45
6f	OPh	4-O_2N-Ph	−5.55	−2.50	3.05
6g	OPh	4-MeO_2S-Ph	−5.45	−1.92	3.53
6h	OPh	4-NC-Ph	−5.47	−2.02	3.45
6i	OPh	4-F_3C-Ph	−5.37	−1.82	3.55
6j	OPh	4-MeO_2C-Ph	−5.28	−1.83	3.45
6k	OPh	4-F-Ph	−5.16	−1.58	3.58
6l	OPh	Ph	−5.11	−1.52	3.59
6m	OPh	4-Me_2N-Ph	−4.66	−1.32	3.34

to the solution. The reaction solution was stirred at −20 °C for 4 h. Then, 20 ml sat. $Na_2S_2O_3$ solution was added and the aqueous phase extracted twice with 40 mL DCM. The combined organic phases were dried over Na_2SO_4, filtered, and the solvent removed *in vacuo*. Purification was carried out by silica chromatography.

General procedure for the Negishi coupling (Route 1):

0.400 g (1 eq) 3-bromoimidazo[1,5-*a*]quinoline 4 was dissolved in 10 mL dry THF under N_2 atmosphere and cooled to −78 °C. 1.2 eq of *n*-BuLi (1.6 M) were slowly added dropwise and the solution was kept at −78 °C for 30 min. 2.5 eq $ZnCl_2$ in dry THF (1 M) were added at −78 °C and then stirred at room temperature for 1 h. 3 mol% of $[Pd_2(dba)_3]\cdot CHCl_3$, 6 mol% of P(*t*-Bu)$_3$ and 2 eq of the chosen coupling bromide were added and the reaction solution was stirred at 70 °C for 20 h. 15 mL conc. $NH_{3(aq)}$ solution was added and the aqueous phase was extracted three times with 20 mL DCM. The combined organic phases were concentrated *in vacuo* and the impure product was purified by silica chromatography.

Procedure for *s*-Triazin formation (Route 2):

0.400 g (1 eq, 1.18 mmol) 3-bromo-1-(phenylether)imidazo[1,5-*a*]quinoline 4b was dissolved in 10 mL dry THF/Et_2O (1 : 1) under N_2 atmosphere and cooled to −78 °C. 0.81 mL (1.1 eq, 1.3 mmol) of *n*-BuLi (1.6 M) were slowly added dropwise and the solution was kept at −78 °C for 30 min. 0.124 g (1.3 eq, 1.53 mmol) of *s*-Triazine was added and the solution was warmed up to room temperature. A yellow participate formed slowly and the solution was stirred at room temperature overnight. 0.05 ml of dest. water was added and the solution stirred for 30 min. Then 20 mL of dest. water and 20 DCM were added and the organic phase separated. The water phase was extracted twice with 20 mL DCM. The combined organic phases were concentrated *in vacuo* and the crude product was dissolved in 20 of dry DCM under N_2 atmosphere and cooled to 0 °C. To this cooled solution 0.321 g (1.2 eq, 1.42 mmol) of DDQ was added and stirred at room temperature overnight. 20 mL dest. water was added and the organic phase was separated. The water phase was extracted twice with 20 mL DCM and the combined organic phases were concentrated *in vacuo*. The crude mixture was purified by silica chromatography (1 : 1 ethyl acetate:*n*-hexane). The product was obtained as a yellow solid (0.287 g, 0.85 mmol, 72% over 2 steps). 1H NMR (400 MHz, $CDCl_3$): δ = 8.94 (s, 2H), 8.62 (d, J = 9.06 Hz, 1H), 8.41 (d, J = 9.58 Hz, 1H), 7.59 (dd, J = 7.83, 1.62 Hz, 1H), 7.45 (ddd, J = 8.69, 7.24, 1.60 Hz, 1H), 7.34 (td, J = 7.55, 1.12 Hz, 1H), 7.31–7.20 (m, 5H), 7.11–7.05 (m, 1H) ppm; 13 C NMR (101 MHz, $CDCl_3$): δ = 167.9, 165.8, 154.4, 147.8, 132.5, 131.8, 130.2, 129.5, 128.6, 126.7, 126.3, 125.4, 125.3, 122.7, 119.2, 118.7, 117.7 ppm; HRMS(ESI): m/z calculated for $C_{20}H_{13}N_5O$ $\{M+Na^+\}$: 362.1012. Found: 362.1014. Elemental Analysis theo.: N = 20.64, C = 70.79, H = 3.86; found: N = 20.61, C = 70.53, H = 3.84.

Supporting Information Summary

Additional references cited within the Supporting Information.[32] Experimental procedures, physical values and spectra for all measured compounds and analytical data of all compounds are provided in the online Supporting Information.

Acknowledgements

Open Access funding enabled and organized by Projekt DEAL.

Conflict of Interests

The authors declare no conflict of interest.

Data Availability Statement

The data that support the findings of this study are available in the supplementary material of this article.

Keywords: Imidazo[1,5-*a*]quinolines · Photoluminescence · Emitter material · Blue luminescence · Nitrogen heterocycles

[1] a) C. W. Tang, S. A. VanSlyke, *Appl. Phys. Lett.* **1987**, *51*, 913–915; b) G. Hong, X. Gan, C. Leonhardt, Z. Zhang, J. Seibert, J. M. Busch, S. Bräse, *Adv. Mater.* **2021**, *33*, e2005630.
[2] a) C. Adachi, M. A. Baldo, S. R. Forrest, S. Lamansky, M. E. Thompson, R. C. Kwong, *Appl. Phys. Lett.* **2001**, *78*, 1622–1624; b) C.-L. Ho, H. Li, W.-Y. Wong, *J. Organomet. Chem.* **2014**, *751*, 261–285; c) H. Nakanotani, T. Higuchi, T. Furukawa, K. Masui, K. Morimoto, M. Numata, H. Tanaka, Y. Sagara, T. Yasuda, C. Adachi, *Nat. Commun.* **2014**, *5*, 4016.
[3] N. C. Giebink, B. W. D'Andrade, M. S. Weaver, P. B. Mackenzie, J. J. Brown, M. E. Thompson, S. R. Forrest, *J. Appl. Phys.* **2008**, *103*, 44509.
[4] a) Y. Im, S. Y. Byun, J. H. Kim, D. R. Lee, C. S. Oh, K. S. Yook, J. Y. Lee, *Adv. Funct. Mater.* **2017**, *27*, 1603007; b) W.-C. Chen, C.-S. Lee, Q.-X. Tong, *J. Mater. Chem. C* **2015**, *3*, 10957–10963.
[5] Z. Xu, J. Gu, X. Qiao, A. Qin, B. Z. Tang, D. Ma, *ACS Photonics* **2019**, *6*, 767–778.
[6] a) R. G. S. Berlinck, R. Britton, E. Piers, L. Lim, M. Roberge, R. Da Moreira Rocha, R. J. Andersen, *J. Org. Chem.* **1998**, *63*, 9850–9856; b) M. S. Malamas, Y. Ni, J. Erdei, H. Stange, R. Schindler, H.-J. Lankau, C. Grunwald, K. Y. Fan, K. Parris, B. Langen, U. Egerland, T. Hage, K. L. Marquis, S. Grauer, J. Brennan, R. Navarra, R. Graf, B. L. Harrison, A. Robichaud, T. Kronbach, M. N. Pangalos, N. Hoefgen, N. J. Brandon, *J. Med. Chem.* **2011**, *54*, 7621–7638; c) A. Kamal, G. Ramakrishna, P. Raju, A. V. S. Rao, A. Viswanath, V. L. Nayak, S. Ramakrishna, *Eur. J. Med. Chem.* **2011**, *46*, 2427–2435; d) D. Kim, L. Wang, J. J. Hale, C. L. Lynch, R. J. Budhu, M. Maccoss, S. G. Mills, L. Malkowitz, S. L. Gould, J. A. DeMartino, M. S. Springer, D. Hazuda, M. Miller, J. Kessler, R. C. Hrin, G. Carver, A. Carella, K. Henry, J. Lineberger, W. A. Schleif, E. A. Emini, *Bioorg. Med. Chem. Lett.* **2005**, *15*, 2129–2134; e) F. Peytam, Z. Emamgholipour, A. Mousavi, M. Moradi, R. Foroumadi, L. Firoozpour, F. Divsalar, M. Safavi, A. Foroumadi, *Bioorg. Chem.* **2023**, *140*, 106831; f) G. Volpi, E. Laurenti, R. Rabezzana, *Molecules* **2024**, *29*, 2668; g) P. A. Chaudhran, A. Sharma, *Crit. Rev. Anal. Chem.* **2022**, 1–18; h) A. K. Bagdi, S. Santra, K. Monir, A. Hajra, *Chem. Comm.* **2015**, *51*, 1555–1575.
[7] a) D. R. Mohbiya, N. Sekar, *ChemistrySelect* **2018**, *3*, 1635–1644; b) F. Yagishita, C. Nii, Y. Tezuka, A. Tabata, H. Nagamune, N. Uemura, Y. Yoshida, T. Mino, M. Sakamoto, Y. Kawamura, *Asian J. Org. Chem.* **2018**, *7*, 1614–1619; c) J. T. Hutt, J. Jo, A. Olasz, C.-H. Chen, D. Lee, Z. D. Aron, *Org. Lett.* **2012**, *14*, 3162–3165; d) Y. Ge, R. Ji, S. Shen, X. Cao, F. Li, *Sens. Actuators B Chem.* **2017**, *245*, 875–881; e) L. Wang, X. Han, G. Qu, Le Su, B. Zhao, J. Miao, *Stem. Cell Res. Ther.* **2018**, *9*, 343.
[8] G. Volpi, B. Lace, C. Garino, E. Priola, E. Artuso, P. Cerreia Vioglio, C. Barolo, A. Fin, A. Genre, C. Prandi, *Dyes Pigm.* **2018**, *157*, 298–304.
[9] a) F. Shibahara, R. Sugiura, E. Yamaguchi, A. Kitagawa, T. Murai, *J. Org. Chem.* **2009**, *74*, 3566–3568; b) G. Volpi, G. Magnano, I. Benesperi, D. Saccone, E. Priola, V. Gianotti, M. Milanesio, E. Conterosito, C. Barolo, G. Viscardi, *Dyes Pigm.* **2017**, *137*, 152–164; c) E. Yamaguchi, F. Shibahara, T. Murai, *J. Org. Chem.* **2011**, *76*, 6146–6158; d) M. Giordano, G. Volpi, C. Garino, F. Cardano, C. Barolo, G. Viscardi, A. Fin, *Dyes Pigm.* **2023**, *218*, 111482; e) G. Colombo, A. Cinco, G. A. Ardizzoia, S. Brenna, *Colorants* **2023**, *2*, 179–193; f) A. Marchesi, S. Brenna, G. A. Ardizzoia, *Dyes Pigm.* **2019**, *161*, 457–463.
[10] G. Volpi, C. Garino, E. Fresta, E. Casamassa, M. Giordano, C. Barolo, G. Viscardi, *Dyes Pigm.* **2021**, *192*, 109455.
[11] F. Shibahara, E. Yamaguchi, A. Kitagawa, A. Imai, T. Murai, *Tetrahedron* **2009**, *65*, 5062–5073.
[12] a) M. D. Weber, C. Garino, G. Volpi, E. Casamassa, M. Milanesio, C. Barolo, R. D. Costa, *Dalton Trans.* **2016**, *45*, 8984–8993; b) F. Yagishita, T.

Kinouchi, K. Hoshi, Y. Tezuka, Y. Jibu, T. Karatsu, N. Uemura, Y. Yoshida, T. Mino, M. Sakamoto, Y. Kawamura, *Tetrahedron* **2018**, *74*, 3728–3733; c) G. A. Ardizzoia, G. Colombo, B. Therrien, S. Brenna, *Ber. dtsch. Chem. Ges. A/B* **2019**, *2019*, 1825–1831; d) S. Durini, G. A. Ardizzoia, B. Therrien, S. Brenna, *New J. Chem.* **2017**, *41*, 3006–3014; e) C. Garino, T. Ruiu, L. Salassa, A. Albertino, G. Volpi, C. Nervi, R. Gobetto, K. I. Hardcastle, *Ber. dtsch. Chem. Ges. A/B* **2008**, *2008*, 3587–3591; f) L. Salassa, C. Garino, A. Albertino, G. Volpi, C. Nervi, R. Gobetto, K. I. Hardcastle, *Organometallics* **2008**, *27*, 1427–1435.

[13] G. Albrecht, C. Rössiger, J. M. Herr, H. Locke, H. Yanagi, R. Göttlich, D. Schlettwein, *Phys. Status Solidi B* **2020**, *257*, 1900677.

[14] G. Albrecht, C. Geis, J. M. Herr, J. Ruhl, R. Göttlich, D. Schlettwein, *Org. Electron.* **2019**, *65*, 321–326.

[15] N. Kulhanek, N. Martin, R. Göttlich, *Eur. J. Org. Chem.* **2024**, *27*, 10.1002/ejoc.202301007.

[16] a) K. C. Langry, *Org. Prep. Proced. Int.* **1994**, *26*, 429–438; b) M. Henze, *Ber. dtsch. Chem. Ges. A/B* **1936**, *69*, 1566–1568.

[17] G. Pelletier, A. B. Charette, *Org. Lett.* **2013**, *15*, 2290–2293.

[18] W. M. Boesveld, P. B. Hitchcock, M. F. Lappert, *J. Chem. Soc., Perkin Trans. 1* **2001**, *9*, 1103–1108.

[19] M. Marner, N. Kulhanek, J. Eichberg, K. Hardes, M. D. Molin, J. Rybniker, M. Kirchner, T. F. Schäberle, R. Göttlich, *RSC Med. Chem.* **2024**, 10.1039/D4MD00086B.

[20] D. F. Eaton, *Pure Appl. Chem.* **1988**, *60*, 1107–1114.

[21] A. M. Brouwer, *Pure Appl. Chem.* **2011**, *83*, 2213–2228.

[22] C.-X. Zhao, T. Liu, M. Xu, H. Lin, C.-J. Zhang, *Chin. Chem. Lett.* **2021**, *32*, 1925–1928.

[23] G. Volpi, E. Priola, C. Garino, A. Daolio, R. Rabezzana, P. Benzi, A. Giordana, E. Diana, R. Gobetto, *Inorganica Chim. Acta* **2020**, *509*, 119662.

[24] C. Rössiger, T. Oel, P. Schweitzer, O. Vasylets, M. Kirchner, A. Abdullahu, D. Schlettwein, R. Göttlich, *Eur. J. Org. Chem.* **2024**, *27*, e202400298.

[25] B. W. D'Andrade, S. Datta, S. R. Forrest, P. Djurovich, E. Polikarpov, M. E. Thompson, *Org. Electron.* **2005**, *6*, 11–20.

[26] J. C. Costa, R. J. Taveira, C. F. Lima, A. Mendes, L. M. Santos, *Opt. Mater.* **2016**, *58*, 51–60.

[27] a) C. Lee, W. Yang, R. G. Parr, *Phys. Rev. B* **1988**, *37*, 785–789; b) P. J. Stephens, F. J. Devlin, C. F. Chabalowski, M. J. Frisch, *J. Phys. Chem.* **1994**, *98*, 11623–11627; c) A. D. Becke, *J. Chem. Phys.* **1993**, *98*, 5648–5652.

[28] A. Schäfer, C. Huber, R. Ahlrichs, *J. Chem. Phys.* **1994**, *100*, 5829–5835.

[29] S. Grimme, J. Antony, S. Ehrlich, H. Krieg, *J. Chem. Phys.* **2010**, *132*, 154104.

[30] a) E. R. Johnson, A. D. Becke, *J. Chem. Phys.* **2006**, *124*, 174104; b) A. D. Becke, E. R. Johnson, *J. Chem. Phys.* **2005**, *123*, 154101.

[31] A. J. Garza, G. E. Scuseria, *J. Phys. Chem. Lett.* **2016**, *7*, 4165–4170.

[32] a) M. S. Wrighton, D. S. Ginley, D. L. Morse, *J. Phys. Chem.* **1974**, *78*, 2229–2233; b) A. E. Sedykh, M. Becker, M. T. Seuffert, D. Heuler, M. Maxeiner, D. G. Kurth, C. E. Housecroft, E. C. Constable, K. Müller-Buschbaum, *Chem. Photo. Chem.* **2023**, *7*, e202200244.

Manuscript received: July 12, 2024
Revised manuscript received: August 6, 2024
Accepted manuscript online: August 12, 2024
Version of record online: October 17, 2024